

# Characterization of Femtosecond Laser-induced Structural Changes in CVD Diamond by Raman Spectroscopy

Keisuke Takabayashi<sup>1</sup>, Kazuki Mimura<sup>2</sup>, Takuro Tomita<sup>2</sup>, and Makoto Yamaguchi<sup>\*1</sup>

<sup>1</sup>Graduate School of Engineering Science, Akita University, Japan

<sup>2</sup>Graduate School of Sciences and Technology for Innovation, Tokushima University, Japan

\*Corresponding author's e-mail: yamaguci@phys.akita-u.ac.jp

Multiple pulses from a femtosecond laser were irradiated onto a diamond grown by chemical vapor deposition, and the dependence of the structural changes of the affected layer on laser parameters was investigated by Raman spectroscopy. A graphite peak was observed in the Raman spectra. The thickness of the graphitized layer was estimated considering the absorption coefficient of graphite. Based on the intensity decrease of diamond peaks, which was the most pronounced change, the dependence of the graphitized layer thickness on the fluence and number of pulses was investigated. As the fluence and/or accumulated number of pulses increased, the thickness of the graphite layer increased. At an accumulated number of pulses of 250 and 2000, the threshold fluence of graphitization was similar to that of laser-induced periodic surface structure formation and smaller than that of ablation. At a fluence below the ablation threshold and a sufficiently large number of pulses, the thickness of the graphite layer remained constant, as determined by the fluence.

DOI: 10.2961/jlmn.2022.02.2005

**Keywords:** femtosecond laser, Raman spectroscopy, CVD diamond, graphitization, laser ablation

## 1. Introduction

Because of their extreme hardness, high thermal conductivity, and chemical inertness, diamonds are used in a wide variety of industrial applications. As the industry has progressed, there is a need to process diamonds with high precision at the micro- and nanoscale. Diamond is the hardest-to-machine material because of its superior properties. Several attempts have been made to fabricate diamonds that satisfy the requirements of machining speed, accuracy, and cost-effectiveness.

Laser processing is one of the most effective methods because of its non-contact nature, free form, high speed, and high accuracy. High-quality laser processing can be achieved by controlling parameters, such as wavelength, pulse duration, and number of pulses [1–2]. A femtosecond (fs) laser has a typical pulse duration of approximately 100 fs, which is shorter than the timescale of electron-lattice interactions [3]. Processing with femtosecond laser pulses provides several advantages, such as small thermal effects [4] and the ability to process transparent materials due to non-linear absorption [5–7], compared with a continuous wave or nanosecond laser.

Laser processing of diamonds, even with femtosecond laser pulses, results in the formation of an affected layer, where diamond-to-graphite transitions and changes in optical properties occur [6–15]. Because the graphitized layer exhibits more degraded properties than the original diamond, the extent of the graphitized layer must be reduced. In the case of synthetic diamonds, which are less expensive than natural diamonds and therefore more suited to industrial applications, the degradation of transmittance has been reported to start early and change gradually [15]. The affected layer can be minimized by optimizing the laser parameters.

However, the relationship between laser-induced structures and laser parameters is not fully understood.

In this study, we present the effects of laser fluence and the accumulated number of pulses on the crystallinity and thickness of the affected layer of synthetic diamonds. A femtosecond laser with several fluences and an accumulated number of pulses was irradiated on a diamond grown by chemical vapor deposition (CVD), and the dependence of the structural changes of the affected layer on the laser parameters was investigated by micro-Raman spectroscopy, which is widely used to characterize carbon-based materials because it is strongly influenced by the crystalline structure and bond disorder. Raman spectra also allow the quantitative estimation of the thickness of the graphitized layer at the measurement point.

## 2. Materials and Methods

A single-crystalline CVD diamond (EDP Corporation, RH553PL) with a size of 5 mm × 5 mm × 0.3 mm was used as the target sample. A Ti:sapphire regenerative amplifier, based on a chirped pulse amplification system and operating at a central wavelength of 800 nm, pulse duration of 130 fs, and repetition rate of 1 kHz (Spectra Physics, Spitfire), was used. The pulse energy irradiated on the sample surface was 20–300 nJ/pulse, controlled by the combination of a polarizing beam splitter and half-wavelength plate. The accumulated number of pulses was 250–2000 shots controlled by a mechanical shutter. The laser beam was focused using an objective lens (20×, numerical aperture of 0.75). The beam radius was evaluated to be 3.0 μm (1/e) using the D<sup>2</sup> method [13]. Accordingly, a fluence of 0.07–1.1 J/cm<sup>2</sup> was determined. Laser irradiation was performed at room temperature under atmospheric conditions.

The irradiated sample surfaces were observed by field-emission scanning electron microscopy (FE-SEM; Hitachi, S-4700).

Micro-Raman spectroscopy was performed at room temperature (Horiba, LabRam HR Evolution) to characterize the laser-induced structure of the sample. The excitation wavelength was set at 355 nm. The wavenumbers were calibrated based on the Raman shift of the first-order phonon peak of single-crystal Si. The wavenumber resolution was approximately  $4\text{ cm}^{-1}$ . A  $40\times$  objective lens was used for focusing, and the diameter of the laser spot was approximately  $1\text{ }\mu\text{m}$ . Therefore, the spatial resolution was estimated to be  $1\text{ }\mu\text{m}$ . The mapping measurements were performed with a spacing of approximately  $0.25\text{ }\mu\text{m}$  at the periphery of the laser-induced area to investigate the most significant changes under each femtosecond laser irradiation condition.

### 3. Results and Discussion

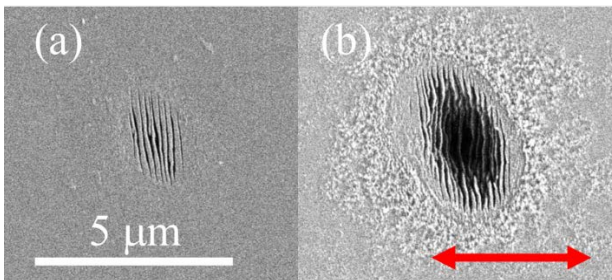
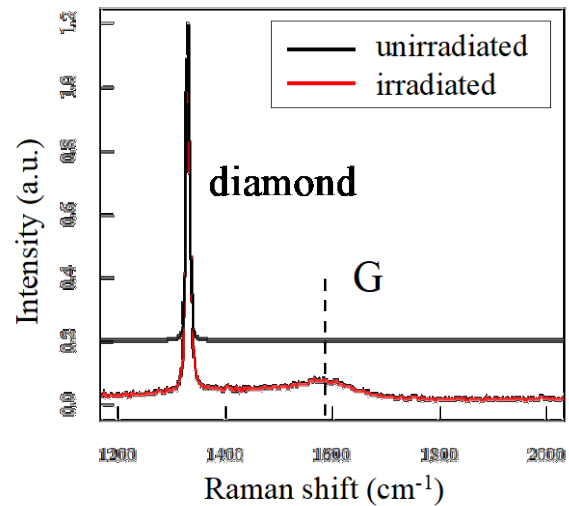


**Fig. 1** SEM image of laser irradiation spot with a fluence of  $0.09\text{ J/cm}^2$  and 2000 shots (a) and a fluence of  $0.18\text{ J/cm}^2$  and 2000 shots (b). The red arrow indicates the direction of femtosecond laser polarization.

Figure 1 (a) shows the SEM image of the laser-irradiated spot with a fluence of  $0.09\text{ J/cm}^2$  and an accumulated number of pulses of 2000 shots. A laser-induced periodic surface structure (LIPSS) [17, 18] was observed in the central region of the irradiation spot, which developed when the accumulated number of pulses ranged from 250 to 500 shots. However, no significant modification was observed on the laser irradiation spot with a fluence of  $0.07\text{ J/cm}^2$  and up to 2000 shots. Therefore, the threshold fluence for LIPSS formation was determined to be approximately  $0.08\text{ J/cm}^2$ .

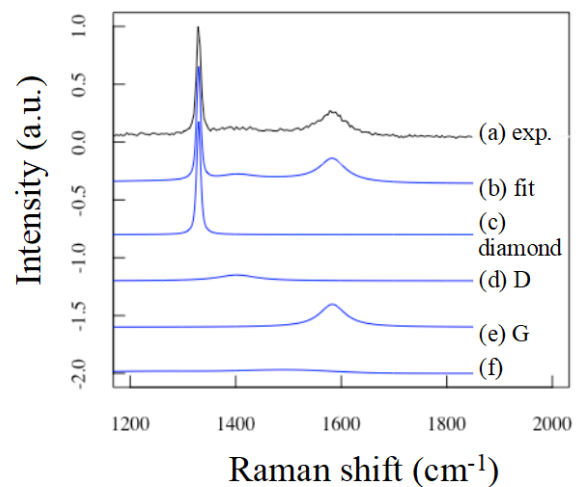
Figure 1 (b) shows the SEM image of the laser-irradiated spot with a fluence of  $0.18\text{ J/cm}^2$  and 2000 shots. A laser-induced crater surrounded by LIPSS was observed. The laser crater was also observed with a fluence of  $0.14\text{ J/cm}^2$  and at an accumulated number of pulses of 2000 shots. However, no crater was observed with a fluence of  $0.11\text{ J/cm}^2$  and up to 2000 shots. Therefore, the threshold fluence for ablation was determined to be approximately  $0.14\text{ J/cm}^2$ .

Figure 2 shows the Raman spectra measured on the unirradiated area and irradiated center of the crater. The spectra were normalized, and the peak observed at  $1332\text{ cm}^{-1}$  was due to diamond [19]. A peak at approximately  $1600\text{ cm}^{-1}$  was only observed at the center of the crater, which was attributed to graphite. The Raman spectrum of graphite has D and G peaks owing to the defects and  $\text{sp}^2$  bonds of carbon, respectively [20]. The observation of the G peak suggests that the graphitization of diamond occurred.



**Fig. 2** Raman spectra measured on the unirradiated area (black) and center of the crater (red). Spectra are normalized to an intensity of approximately  $1332\text{ cm}^{-1}$ .

Regression analysis was performed for each point in the Raman spectra obtained from the mapping measurements. The Levenberg-Marquardt algorithm was used (R language, Minpack library). An example of fitting of the Raman spectrum is shown in Fig. 3, which was measured at the center of the crater with a fluence of  $1.1\text{ J/cm}^2$  and 2000 shots. In Fig. 3, curve (a) shows a typical Raman spectrum at the crater center; curve (b) shows the fitting result for curve (a); and curves (c)–(f) show the fitting elements used for curve (b). A pseudo-Voigt function, which is a combination of the Gaussian and Lorentzian functions, was used for fitting the diamond peak. The peaks due to graphite included D, G, and two additional peaks. Lorentzian function was used for fitting the D peak, pseudo-Voigt function for the G peak, and Gaussian function for the two additional peaks close to  $1220\text{ cm}^{-1}$  and  $1500\text{ cm}^{-1}$ . A linear function was used as the baseline. The full width at half maximum of the G peak was about approximately  $59.7\text{ cm}^{-1}$ .



**Fig. 3** Fitting results of the Raman spectrum on the laser-induced area of CVD diamond. Spectrum (a), fitting result (b), and the decomposed elements (c)–(f) are displayed.

Figure 4 (a) shows the spatial distribution of the relative intensity of the diamond peak to the unirradiated diamond peak intensities at a fluence of 0.11 J/cm<sup>2</sup> and 250 shots. Black represents the same intensity as the unirradiated area, and black, blue, and yellow represent decreasing intensities in that order. The relative intensity of diamond shows a gradual decrease toward the center of irradiation with a decline of approximately 36% at the center.

Figure 4 (b) shows the spatial distribution of the relative intensity of the G peak to the intensity of the unirradiated diamond peak at a fluence of 0.11 J/cm<sup>2</sup> and 250 shots. Black indicates that the G peak intensity is 0, and black, blue, and yellow indicate increasing G peak intensities in that order. The comparison of Figs. 4 (a) and (b) indicates that the decrease in the relative intensity of diamond correlates with the increase in the relative intensity of graphite.

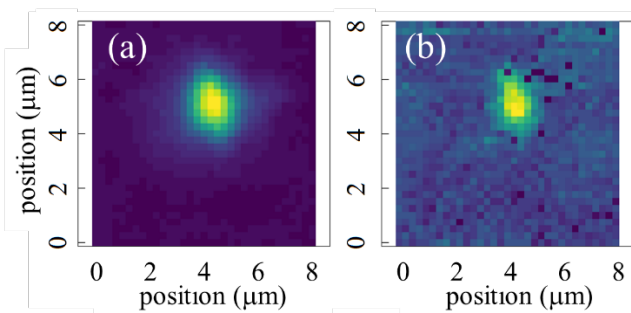


**Fig. 4** Spatial distributions of the relative intensity of diamond (a) and G peaks (b) at a fluence of 0.11 J/cm<sup>2</sup> and 250 shots. The intensities of diamond and G peak are normalized by the intensity of the unirradiated diamond, and decrease and increase toward the irradiation center, respectively.

Laser irradiation may cause a structural change in the diamond surface layer to yield a structure with a large absorption coefficient. If this layer is on the diamond surface, the intensity of the excitation light and Raman scattered light decreases owing to absorption, and the relationship between the thickness of the layer and intensity of diamond is given by the following [21, 22]:

$$t = \frac{1}{2\alpha} \log(I_{\text{dia},0}/I_{\text{dia}}), \quad (1)$$

where  $t$  and  $\alpha$  are the thickness of the absorption layer and absorption coefficient, respectively.  $I_{\text{dia},0}$  and  $I_{\text{dia}}$  are the peak intensities of the unirradiated diamond and irradiated layer, respectively. In this model, it is assumed that the absorption coefficients of the Raman-scattered light and excitation light remain the same.

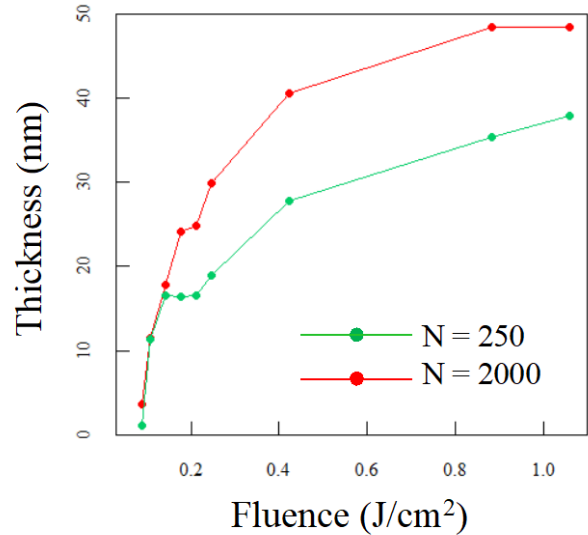


**Fig. 5** Thickness of the graphitized layer against fluence with 250 and 2000 shots. The layer at 2000 shots is thicker than that at 250 shots.

The dependence of the thickness of the affected layer on fluence is shown in Fig. 5 and was calculated using eq. (1). Because the G peak was observed by femtosecond laser irradiation, the affected layer was considered to be graphitized. Therefore, the absorption coefficient of graphite was considered in eq. (1) [23]. The graphitized layer thickness increased with fluence, up to about 50 nm at a fluence of 1.1 J/cm<sup>2</sup> and 2000 shots. The threshold fluence for graphitization was estimated to be approximately 0.08 J/cm<sup>2</sup>, both at 250 and 2000 shots.

The G peak was not observed at a fluence of 0.09 J/cm<sup>2</sup>, though it was above the threshold fluence for graphitization determined in Fig. 5. This is because the graphite layer formed was very thin (less than 5 nm). Even graphitization effects that are too small to be observed as G peaks can be confirmed by examining the intensity of diamond.

Figure 6 shows a semi-log plot of the graphitized layer thickness against the accumulated number of pulses of 250, 500, 1000, and 2000 shots. The dashed lines are eye guides. The points on or near a dashed line are the experimental results at the corresponding fluence, with thicknesses increasing in the order of fluences of 0.09, 0.11, 0.21, and 1.1 J/cm<sup>2</sup>. There was a linear increase in the thickness with respect to the logarithm of the accumulated number of pulses. The slope increases as the fluence increases. The intersection of the dashed line with the x-axis at  $t = 0$  ( $N_0$ ) decreased as the fluence increased. At a fluence of 1.1 J/cm<sup>2</sup>, which is the maximum fluence under our experimental conditions,  $N_0$  is approximately equal to 1. It is estimated that graphitization occurred from the first pulse at this fluence.

The fluences of 0.09 and 0.11 J/cm<sup>2</sup> are below the threshold fluence for ablation as shown in Fig. 6. At such fluences and for sufficiently large numbers of pulses, the thickness of the graphitized layer is constant as determined by the fluence.

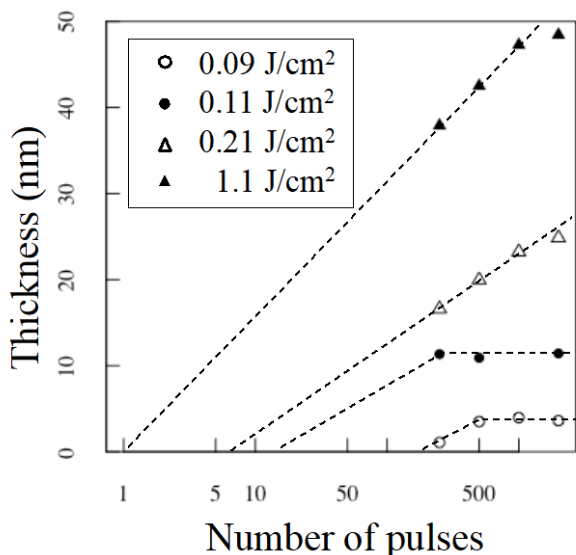


**Fig. 6** Semi-log plot of graphitized layer thickness against the accumulated number of pulses of 250, 500, 1000, and 2000 shots at fluences of 0.09, 0.11, 0.21, and 1.1 J/cm<sup>2</sup>. The layer was thicker at a higher fluence.

#### 4. Conclusion

Femtosecond laser pulses operating at a central wavelength of 800 nm, pulse duration of 130 fs, and repetition rate of 1 kHz were irradiated onto a single-crystalline CVD diamond with fluences ranging from 0.07 to 1.1 J/cm<sup>2</sup> and accumulated number of pulses from 250 to 2000. The dependence of the structural changes in the CVD diamond on the fluence and accumulated number of pulses was investigated by Raman spectroscopy. The emergence of a G peak due to graphite and a decrease in the diamond peak intensity were observed in the laser-irradiated area. We assumed that these Raman spectral changes were due to optical absorption by the affected layer and estimated the thickness of the affected layer. As a G peak was observed, we assumed that the affected layer was graphitized and considered the absorption coefficient of graphite. The graphitized layer was formed at a fluence of approximately 0.08 J/cm<sup>2</sup>, which is comparable to that of LIPSS formation in the range of 250 to 2000 shots. The thickness of the graphitized layer increased as the fluence increased and was approximately 50 nm at a fluence of 1.1 J/cm<sup>2</sup> and 2000 shots. The thickness also increased as the accumulated number of pulses increased but remained constant at fluences below the ablation threshold.

#### Acknowledgments

This study was conducted at the Institute for Solid State Physics, University of Tokyo. This study was supported by the AMADA FOUNDATION.

#### References

[1] E. Ludvigsen, N. R. Pedersen, X. Zhu, R. Marie, D. M. A. Mackenzie, J. Emnéus, D. H. Petersen, A. Kristensen, and S. S. Keller: *Micromachines*, 12, (2021) 564.

- [2] X. Zhu, J. Engelberg, S. Remennik, B. Zhou, J. N. Pedersen, P. U. Jepsen, U. Levy, and A. Kristensen: *Nano Lett.*, 22, (2022) 2786.
- [3] J. R. Goldman and J. A. Prybyla: *Phys. Rev. Lett.*, 72, (1994) 1364.
- [4] B. N. Chichkov, B. N. Chichkov, C. Momma, S. Nolte, F. Y. Alvensleben, and A. Tünnermann: *Appl. Phys. A*, 63, (1996) 109.
- [5] Y. Liao, Y. Shen, L. Qiao, D. Chen, Y. Cheng, K. Sugioka, and K. Midorikawa: *Opt. Lett.*, 38, 2, (2013) 287.
- [6] F. Ladieu, P. Martin, and S. Guizard: *Appl. Phys. Lett.*, 81, (2002) 957.
- [7] P. Boerner, M. Hajri, N. Ackerl, and K. Wegener: *J. Laser Appl.*, 31, (2019) 022202.
- [8] V. V. Kononenko, A. A. Khomich, A. V. Khomich, R. A. Khmel'nitskii, V. M. Gololobov, M. S. Komlenok, A. S. Orekhov, A. S. Orekhov, and V. I. Konov: *Appl. Phys. Lett.*, 114, (2019) 251903.
- [9] G. Dumitru, V. Romano, H. P. Weber, S. Pimenov, T. Kononenko, J. Hermann, S. Bruneau, Y. Gerbig, and M. Shupegiin: *Diam. Relat. Mater.*, 12, (2003) 1034.
- [10] T. V. Kononenko, V. V. Kononenko, S. M. Pimenov, E. U. Zavedoev, V. I. Konov, V. Romano, and G. Dumitru: *Diam. Relat. Mater.*, 14, (2005) 1368.
- [11] P. W. Butler-Smith, D. A. Axinte, M. Pacella, and M. W. Fay: *J. Mater. Proc. Tech.*, 213, (2013) 194.
- [12] L. Zhao, C. Song, J. Zhang, Y. Huang, C. Zhang, Y. Liu, B. Dong, Z. Xu, G. Li, and T. Sun: *Appl. Surf. Sci.*, 578, (2021) 151995.
- [13] S. Odake, H. Ohfuji, T. Okuchi, H. Kagi, H. Sumiya, and T. Irifune: *Diam. Relat. Mater.*, 18, (2009) 877.
- [14] T. Okada, T. Tomita, T. Ueki, Y. Masai, Y. Bando, and Y. Tanaka: *Jpn. J. Appl. Phys.*, 56, (2017) 112701.
- [15] T. V. Kononenko, M. S. Komlenok, S. M. Pimenov, V. Romano, V. P. Pashinin and V. I. Konov: *Appl. Phys. A*, 90, (2008) 645.
- [16] J. M. Liu: *Opt. Lett.*, 7, (1982) 196.
- [17] P. Calvani, A. Bellucci, M. Girolami, S. Orlando, V. Valentini, A. Lettino, and D. M. Trucchi: *Appl. Phys. A*, 117, (2014) 25.
- [18] E. Granados, M. Martinez-Calderon, M. Gomez, A. Rodriguez, and S. M. Olaizola: *Opt. Express*, 25, 13, (2017) 15330.
- [19] R. S. Krishnan: *Nature*, 155, (1945) 171.
- [20] A. C. Ferrari and J. Robertson: *Phil. Trans. R. Soc. Lond. A*, 362, (2004) 2477.
- [21] S. Shivaraman, M. V. S. Chandrashekhar, J. J. Boeckl, and M. G. Spencer: *J. Electron. Mater.*, 38, (2009) 725.
- [22] J. Bonse, K. W. Brzezinka, and A. J. Meixner: *Appl. Surf. Sci.*, 221, (2004) 215.
- [23] V. I. Konov: *Laser Photonics Rev.*, 6, (2012) 739.

(Received: June 25, 2022, Accepted: August 28, 2022)